Optica Applicata, Vol. LII, No. 4, 2022
DOI: 10.37190/oa220403

Strain measurement based on fixed wavelength transmission of tapered long-period fiber grating

Yong Tang, Hao Zhang, Li Zhang, Xin Feng Yu, Yun Feng Bai*

Key Laboratory of Micro Nano Optoelectronic Devices and Intelligent Perception Systems, School of Electronic Information and Engineering, in Yangtze Normal University, Chongqing, 408100, China

*Corresponding author: baiyunfeng@126.com

This paper studies the relationship between transmission intensity and strain based on tapered long -period fiber grating at a fixed wavelength. In experiments, tapered long-period fiber grating was prepared by the electric melting method. Experimental results show that two resonance peaks appeared at 1482 and 1537 nm, respectively. Here is the elaboration of the relationship between the resonant wavelength and the strain, its wavelength-strain sensitivity is 20 pm/με, and the linearity was negative. Then our next study was about the relationship between transmission intensity and strain at a fixed wavelength. The results show that the transmission intensity at a fixed wavelength is related to the exponent with strain. The coupled-mode theory is applied to simulate the relationship between fixed wavelength and strain. The simulation results matched the experimental results. Two fixed wavelength transmission intensity ratio was used, and the ratio showed a linear relationship with the strain, and the slope is –0.018 dB/με. Therefore, within the 0.01% resolution of our detector, we could resolve a 0.16 με strain change. We can select the appropriate light source and detector to achieve higher measurement accuracy. Thus, there is a great potential in fiber grating strain sensors.

Keywords: tapered long-period fiber grating, strain sensors, fixed dual-wavelength ratio.

1. Introduction

Because of their weak electromagnetic interference, small size, lightweight, and other advantages [1,2], fiber optic sensors have been successfully used in aerospace chemistry, industrial power, water and electricity, shipbuilding, mining, and other industries [3,4]. For now, optical fiber sensors are mainly divided into fiber Bragg grating (FBG) sensors [5,6] and long-period fiber grating (LPFG) sensors. Since the coupling mode of FBG is the mutual coupling between the fiber core and the fiber core, while LPFG is the coupling between the fiber core and the cladding, LPFG is more sensitive to the changes of the external environment and has been extensively studied. The tapered long-period fiber grating (T-LPFG) sensor is one kind of them, and it is easy to be produced. It plays a pre-eminent role in the detection of temperature [7–9], strain [10,11],

bending [12], refractive index [13], and other physical quantities [14]. However, the current sensing modes of LPFG are based on the linear relationship between the resonance wavelength and the external environment. In 2006, WANG *et al*. studied a highly sensitive LPFG strain sensor, and its strain sensitivity was 0.0076 nm/με [10]. In 2017, SUN *et al*. made a helical long-period fiber grating temperature sensor using the welding mechanism, and its sensitivity was 69.9 pm/°C [8]. In 2021, ALUSTIZA *et al*. studied a strain sensor with a sensitivity of 0.00119 nm/με [15]. Since all the sensing modes of LPFG are based on the linear relationship between the resonance wavelength and the external environment, it is so important to monitor the change of the resonance wavelength during measurement. Generally, a spectrometer is used to monitor wavelength change. However, the spectrometer is costly and is not conductive to application, so the ratiometric demodulation techniques are invented, There are two forms of ratiometric demodulation techniques. The edge filter: employs an edge filter to convert the wavelength measurement into the intensity ratio [16,17]. In 2013, HISHIKI *et al*. studied a large bent fiber loss filter and used a ratio system to demodulate a fiber grating strain sensor [14]. This method's principle is to convert the wavelength measurement into the signal strength ratio measurement by using the transition region of the response transmitted by the edge filter. The other is based on the resonance wavelength and does not change with external influences [18], so the transmission strength of the resonance wavelength can be used in strain sensors.

Below, a T-LPFG is prepared by a welding machine. The relationship between transmission intensity and strain at fixed wavelength is more elaborated. The experimental results show that the transmission intensity at a fixed wavelength is related to the exponent with strain. Further, the relationship between the fixed dual-wavelength ratio and the strain is shown, and it shows a good linear relationship. This experimental phenomenon has great potential in fiber grating strain sensors.

2. Preparation method of T-LPFG

T-LPFG was fabricated by an electric heating method, and the optical fiber cladding of about 5 cm was peeled off with wire strippers (the single-mode fiber adopts the standard model produced by Wuhan Changfei Company, the core diameter is 9 μm, the cladding diameter is 125 μm, Welding machine number: Yoko kawa - AQ6370D). Wipe the stain on the exposed fiber with alcohol-soaked cotton, then place the exposed fiber between the electrodes of the fiber fusion machine. Figure 1 shows that the parameters of the designed T-LPFG with the waist diameter is 90 μm, the length is 0.1 μm and the length of the left and right cones is 0.2 μm. Then, the multi-function fiber fusion machine program is set to pull cone mode. Motor parameters are set as follows: the left motor moves to the left, the speed is set to 0.3 mm/s, the right motor moves to the left, the speed is set to 0.17 mm/s, the running time is 3.85 s.

After pulling the cone each time, the computer controls both the left and right stepping motors of the optical fiber fuse machine to move synchronously, so that the optical fiber moves at a fixed length of 0.1 mm each time. Then the above process is repeated,

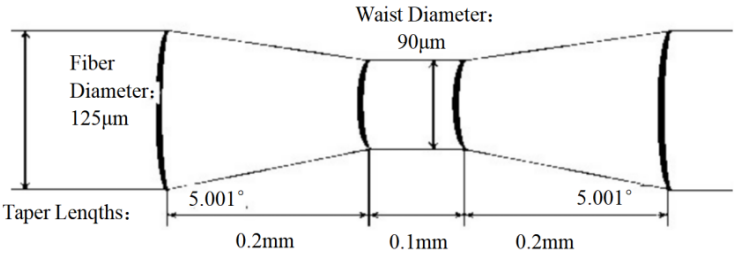

Fig. 1. Parameter for the T-LPFG.

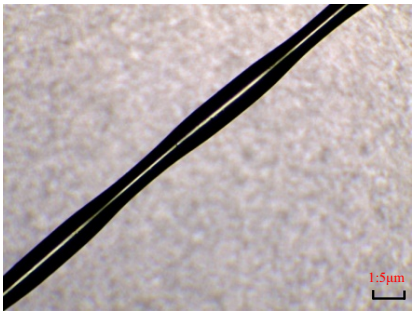

Fig. 2. Micrograph of the T-LPFG.

and real-time observation of the transmission spectra is done until there are two pronounced loss peaks and then it stops. With the microscope, the fiber shape after taper drawing was distinct, as shown in Fig. 2.

3. Results and the discussion

The transmission spectrum of the T-LPFG was measured using broadband light sources (1400–1640 nm) and the spectrometer. Fix the left fixture, and move the right fixture 0.01 mm to the right each time. The strain formula is

$$\varepsilon = \frac{\Delta L}{L} \times 10^{-6} \tag{1}$$

According to the above experimental description, L is 5 cm, ΔL is 0.1 mm, then each time the strain is 200 με. The transmission spectra of 0, 400, 800 and 1200 με are shown in Fig. 3. From Fig. 3, we can see that as the strain increases, the two resonance wavelengths show a redshift, the same as the early reported [19].

According to the coupled-mode theory of LPFG, the coupling of the fundamental mode in the fiber core to the forward propagating cladding mode leads to the appearance of a loss peak. For general LPFG, the phase-matching condition can be described as [20]

$$n_{\mathrm{N}} = n_{\mathrm{F}} - \frac{\lambda}{\Lambda} \tag{2}$$

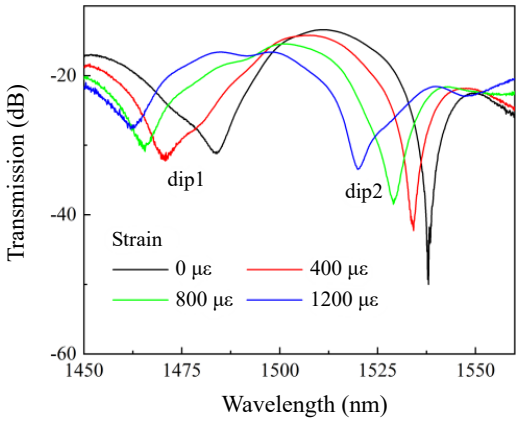

Fig. 3. The transmission spectrum of the 0, 400, 800, and 1200 με.

If n order harmonics are considered, the pattern selection rule can be described as [21]

$$n_{\mathrm{N}} = n_{\mathrm{F}} - \frac{n\lambda}{\Lambda} \tag{3}$$

where n is the harmonic order, n_{F} and n_{N} are the effective refractive index of the fundamental mode and cladding modes, respectively. λ is the resonant wavelength of the LPFG. Based on Eq. (3), two resonant peaks are calculated, one is the fourth-order coupling between the fundamental mode and the LP_{14} caldding mode, and the other is the seventh-order coupling between the fundamental mode and the LP_{18} caldding mode.

The relationship between resonance wavelength and strain is elaborated, as shown in Fig. 4. The resonance wavelength is the linear variation with strain, and its linear fitting accuracy is 0.98166. Its slope is –0.02 nm/με, that is, the wavelength changes 0.02 nm for every 1 με, which is about ten times higher than in Ref. [13]. However,

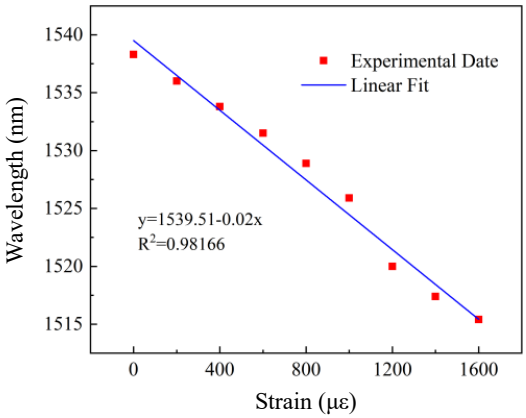

Fig. 4. Relationship between resonance wavelength and strain.

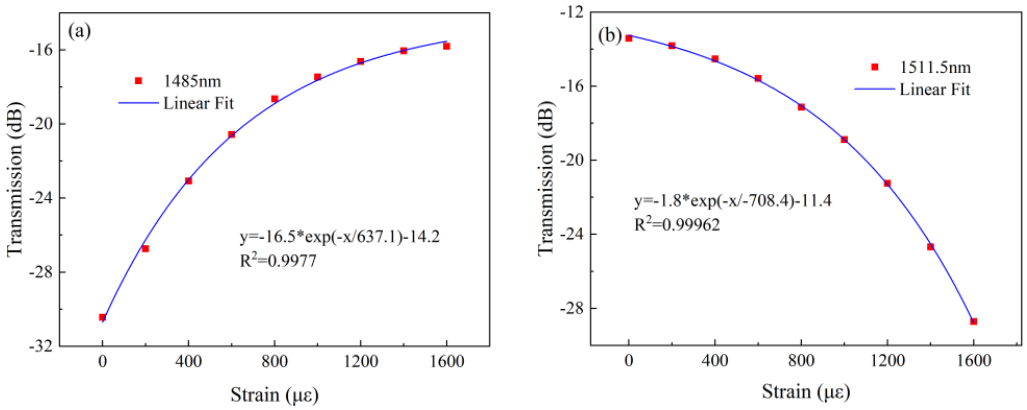

Fig. 5. Relationship between the transmission intensity and fixed wavelength: (a) 1485 nm, (b) 1511.5 nm.

because of the fluctuations in spectral data, the resonance wavelength is quite not easy to be measured, which will affect the fitting accuracy. So we developed a new method to measure strain. As can be seen from Fig. 3, the transmission intensity varies regularly with the strain at a certain wavelength. We chose the fixed wavelength of 1485 and 1511.5 nm and found that the transmission strength and strain showed an exponential relationship. The fitting accuracy is 0.9977 and 0.99962, respectively. It indicates that the transmission intensity at a fixed wavelength can be used to measure strain.

The coupled-mode theory was used to simulate the relationship between transmission intensity of a fixed wavelength and strain of T-LPFG [4,22,23].

$$A = \cos^2(\sqrt{k^2+\hat{\sigma}^2}\,z) + \frac{\hat{\sigma}^2}{k^2+\hat{\sigma}^2}\sin^2(\sqrt{k^2+\hat{\sigma}^2}\,z) \tag{4}$$

$$\hat{\sigma} = \delta + \frac{\sigma_{11}-\sigma_{22}}{2} \tag{5}$$

$$k = \sigma(z)\frac{2\pi}{\lambda}\sqrt{\frac{\pi b}{Z_0 n_2\sqrt{1+2b\Delta}}}\,\frac{n_1^2 u_1}{u_1^2 - V^2(1-b)/a_1^2}\left(1+\frac{\sigma_2\xi_0}{n_1^2}\right)$$
$$\times E_{1\nu}^{\mathrm{cl}}\left[u_1 J_1(u_1 a_1)\frac{J_0(V\sqrt{1-b})}{J_1(V\sqrt{1-b})}\right] - \frac{V\sqrt{1-b}}{a_1}J_0(u_1 a_1) \tag{6}$$

$$b = \frac{n_{\mathrm{eff}}^2 - n_2^2}{n_1^2 - n_2^2} \tag{7}$$

$$\Delta = \frac{n_1 - n_2}{n_1} \tag{8}$$

$$V = \frac{2\pi}{\lambda} a_1 \sqrt{n_1^2 - n_2^2} \tag{9}$$

$$\xi_0 = \frac{1}{\sigma_2} \frac{u_2\left(JK - \dfrac{\sigma_1\sigma_2 u_{21}u_{32}}{n_2^2 a_1 a_2}\right) p_1(a_2) - Kq_1(a_2) + Jr_1(a_2) - \dfrac{1}{u_2} s_1(a_2)}{-u_2\left(\dfrac{u_{32}}{n_2^2 a_2} J - \dfrac{u_{21}}{n_1^2 a_1} K\right) p_1(a_2) + \dfrac{u_{32}}{n_1^2 a_1} q_1(a_2) + \dfrac{u_{21}}{n_1^2 a_1} r_1(a_2)} \tag{10}$$

where A is the transmission rate, $\hat{\sigma}$ is DC self-coupling coefficient, k is an AC coupling coefficient, δ is the detuning, λ is the wavelength, v is the fringe visibility of the index change, z is the length of T-LPFG, n_1 and n_2 are the refractive index of the fiber core and the cladding, respectively, n_{eff} is the effective refractive index of the fundamental mode, and $\sigma(z)$ is the slowly varying envelope of the grating. The effective elasto-optic coefficient of the grating is 0.222678. The remaining quantities can be obtained from Ref. [21].

Figure 6 shows the coincidence of experimental data and theoretical data after adding 15.8 dB. This indicates that the strain measurement with the transmission intensity of fixed wavelength is fully supported theoretically. Due to the slight deformation of the fiber during processing there is a difference of about 15.8 dB between the measured results and the simulated results, resulting in the loss of light from the core to the stripping. But there is a difficulty in measuring strain with transmitted light intensity, and the difficulty is that there is a fluctuation of light source intensity. As we all know, the dual-wavelength ratio method is usually adopted to the influence of light intensity elimination [24].

The influence of the light source will be eliminated by dividing the transmission intensity of two fixed wavelengths. In addition, a perfect linear relationship is obtained

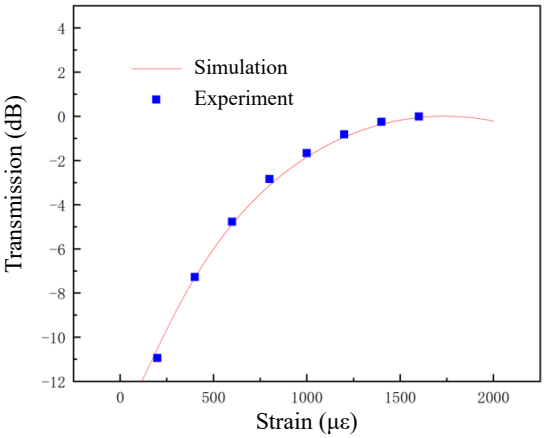

Fig. 6. The diagram between theoretical simulation and experiment.

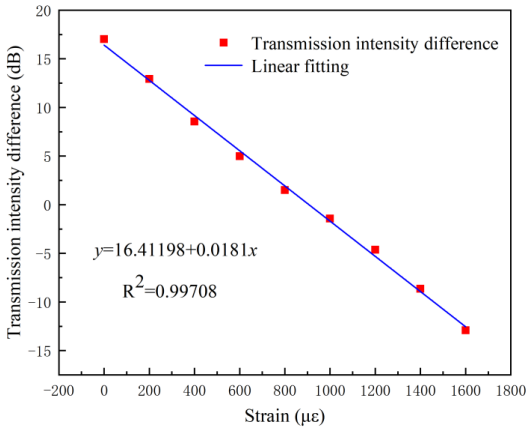

Fig. 7. The relationship between transmission intensity difference and strain.

as shown in Fig. 7. Compared with the exponential relationship, the strain measurement by linear relationship is easier, where $R^2 = 0.99708$, the slope is –0.0181 dB/με. It also proves that the method of measuring strain using the dual-wavelength projection ratio is feasible, and it has great application potential in strain sensors. When the fixed dual-wavelength transmission intensity ratio is performed, the transmission intensity ratio changes to 99.9%, and the strain change of 0.16 με can be detected by using a 0.01% detector. In 2000, GRUBSKY and FEINBERG [18] used the same method to calculate the sensitivity, and also adopted the light intensity as the parameter of strain measurement, but the sensitivity is 1 με. And the sensitivity of this report is increased by an order of magnitude compared with Ref. [8]. The sensitivity of transmission intensity and strain at fixed wavelength is much higher than that of resonance wavelength and strain. So high-sensitivity detectors can be used to improve the sensitivity of the sensor. It has great potential applications in strain sensors.

4. Conclusions

A multi-functional optical fiber welding machine is used to manufacture T-LPFG, and the light intensity is used as a parameter to carry out both the theoretical research and experimental measurement of strain. It is found that the theoretical simulation matches the experimental data. The experimental function relation between fixed wavelength transmission light intensity and strain improves the sensitivity of the strain sensor. To reduce the requirements for light source stability, a dual-wavelength transmission intensity ratio is advised to measure strain. In addition, the dual-wavelength ratio method does not need to be limited by the resonance wavelength, and in theory, many wavelengths can be selected for measurement. The results show that the dual-wavelength transmission intensity ratio has a linear ship with strain, and the measurement accuracy can reach 0.16 με. Moreover, the sensitivity is further heightened by a better high-precision detector. This work was inspired by the significance of the fiber grating sensor.

Acknowledgment
This work was supported by the Science and Technology Research Program of Chongqing Science and Technology Commission (KJQN20200142) and (KJZDM202001401); Shale Gas Optical Fiber Intelligent Sensing, Technology University Innovation Research Group (CXQT20027).

References

[1] HILL K.O., FUJII Y., JOHNSON D.C., KAWASAKI B.S., *Photosensitivity in optical fiber waveguides: application to reflection filter fabrication*, Applied Physics Letters **32**(10), 1978, pp. 647–649, DOI: 10.1063/1.89881.

[2] LEE B., *Review of the present status of optical fiber sensors*, Optical Fiber Technology **9**(2), 2003, pp. 57–79, DOI: 10.1016/S1068-5200(02)00527-8.

[3] LEE B.H., LIU Y., LEE S.B., CHOI S.S., JANG J.N., *Displacements of the resonant peaks of a long-period fiber grating induced by a change of ambient refractive index*, Optics Letters **22**(23), 1997, pp. 1769–1771, DOI: 10.1364/OL.22.001769.

[4] LAM D.K.W., GARSIDE B.K., *Characterization of single-mode optical fiber filters*, Applied Optics **20**(3), 1981, pp. 440–445, DOI: 10.1364/AO.20.000440.

[5] ZAGORULKO K.A., KRYUKOV P.G., LARIONOV YU.V., RYBALTOVSKY A.A., DIANOV E.M., CHEKALIN S.V., MATVEETS YU.A., KOMPANETS V.O., *Fabrication of fiber Bragg gratings with 267 nm femtosecond radiation*, Optics Express **12**(24), 2004, pp. 5996–6001, DOI: 10.1364/OPEX.12.005996.

[6] LAU K.-T., YUAN L., ZHOU L.-M., WU J.S., WOO C.-H., *Strain monitoring in FRP laminates and concrete beams using FBG sensors*, Composite Structures **51**(1), 2001, pp. 9–20, DOI: 10.1016/S0263-8223(00)00094-5.

[7] HAO Z., YU X.F., YU Z., BAI Y.F., TIAN Y.Q., DANG S., *Method for temperature measurement of taper long-period fiber Bragg grating*, Optical Engineering **60**(5), 2021, article no. 050501, DOI: 10.1117/1.OE.60.5.050501.

[8] SUN B., WEI W., LIAO C.R., ZHANG L., ZHANG Z.X., CHEN M.-Y., WANG Y.P., *Automatic arc discharge-induced helical long period fiber gratings and its sensing applications*, IEEE Photonics Technology Letters **29**(11), 2017, pp. 873–876, DOI: 10.1109/LPT.2017.2693361.

[9] RAO Y.-J., RAN Z.-L., LIAO X., DENG H.-Y., *Hybrid LPFG/MEFPI sensor for simultaneous measurement of high-temperature and strain*, Optics Express **15**(22), 2007, pp. 14936–14941, DOI: 10.1364/OE.15.014936.

[10] WANG Y.-P., XIAO L., WANG D.N., JIN W., *Highly sensitive long-period fiber-grating strain sensor with low temperature sensitivity*, Optics Letters **31**(23), 2006, pp. 3414–3416, DOI: 10.1364/OL.31.003414.

[11] ZHOU D.-P., WEI L., LIU W.-K., LIU Y., LIT J.W.Y., *Simultaneous measurement for strain and temperature using fiber Bragg gratings and multimode fibers*, Applied Optics **47**(10), 2008, pp. 1668–1672, DOI: 10.1364/AO.47.001668.

[12] BAI Y.F., HE Z.L., BAI J.Y., DANG S.H., *Axial strain measurement based on dual-wavelength ratio for helical long-period grating*, IEEE Sensors Letters **4**(11), 2020, article no. 1500803, DOI: 10.1109/LSENS.2020.3035519.

[13] REN K., REN L., LIANG J., KONG X., JU H., WU Z., *Highly strain and bending sensitive microtapered long-period fiber gratings*, IEEE Photonics Technology Letters **29**(13), 2017, pp. 1085–1088, DOI: 10.1109/LPT.2017.2702573.

[14] HISHIKI K., LI H., YIN S., *Phase-shift formed in a tapered long period fiber grating and its application to simultaneous measurements of temperature and refractive-index*, Proc. SPIE 8847, Photonic Fiber and Crystal Devices: Advances in Materials and Innovations in Device Applications VII, 88470O (25 September 2013), DOI: 10.1117/12.2021684.

[15] ALUSTIZA D., MINEO M., RUSSO N.A., *Characterization of long period gratings manufactured with fiber optic fusion splicer for sensor development*, Latin American Applied Research **51**(1), 2021, pp. 21–26, DOI: 10.52292/j.laar.2021.544.

[16] Melle S.M., Liu K., Measures R.M., *A passive wavelength demodulation system for guided-wave Bragg grating sensors*, IEEE Photonics Technology Letters **4**(5), 1992, pp. 516–518, DOI: 10.1109/68.136506.

[17] Lobo Ribeiro A.B., Ferreira L.A., Tsvetkov M., Santos J.L., *All-fibre interrogation technique for fibre Bragg sensors using a biconical fibre filter*, Electronics Letters **32**(4), 1996, pp. 382–383, DOI: 10.1049/el:19960260.

[18] Grubsky V., Feinberg J., *Long-period fiber gratings with variable coupling for real-time sensing applications*, Optics Letters **25**(4), 2000, pp. 203–205, DOI: 10.1364/OL.25.000203.

[19] Zhang C.-L., Gong Y., Zou W.-L., Y. Wu, Rao Y.-J., Peng G.-D., Fan X.D., *Microbubble-based fiber optofluidic interferometer for sensing*, Journal of Lightwave Technology **35**(13), 2017, pp. 2514–2519, DOI: 10.1109/JLT.2017.2696957.

[20] Bhatia V., Vengsarkar A.M., *Optical fiber long-period grating sensors*, Optics Letters **21**(9), 1996, pp. 692–694, DOI: 10.1364/OL.21.000692.

[21] Löfving B., Härd S., *Optical switching with two FLC SLMs*, Optics Communications **174**(1–4), 2000, pp. 81–90, DOI: 10.1016/S0030-4018(99)00711-7.

[22] Mizrahi V., Sipe J.E., *Optical properties of photosensitive fiber phase gratings*, Journal of Lightwave Technology **11**(10), 1993, pp. 1513–1517, DOI: 10.1109/50.249888.

[23] Erdogan T., *Cladding-mode resonances in short- and long-period fiber grating filters*, Journal of the Optical Society of America A **14**(8), 1997, pp. 1760–1773, DOI: 10.1364/JOSAA.14.001760.

[24] El-Damak A.R., Chang J., Jian S., Xu C., Gu X., *Dual-wavelength, linearly polarized all-fiber laser with high extinction ratio*, IEEE Photonics Journal **5**(4), 2013, article no. 1501406, DOI: 10.1109/JPHOT.2013.2276991.

Received September 6, 2021
in revised form January 27, 2022